Bioorganic & Medicinal Chemistry 16 (2008) 7301–7309

Contents lists available at ScienceDirect

Bioorganic & Medicinal Chemistry

journal homepage: www.elsevier.com/locate/bmc

Synthesis, DNA binding, and cytotoxic evaluation of new analogs of diallyldisulfide, an active principle of garlic

Santosh Kumar Rai [a], Meenakshi Sharma [b], Manisha Tiwari [a,*]

[a] Dr. B.R. Ambedkar Center for Biomedical Research, University of Delhi, Delhi 110007, India
[b] Department of Biomedical and Pharmaceutical Sciences, University of Rhode Island, RI 02881, USA

ARTICLE INFO

Article history:
Received 9 May 2008
Revised 16 June 2008
Accepted 17 June 2008
Available online 20 June 2008

Keywords:
Diallyldisulfide
Drug–DNA interaction
Circular dichroism
Differential scanning calorimetry

ABSTRACT

Diallyldisulfide (DADS), an active principle of garlic (*Allium sativum*) is known for its antihyperlipidemic properties. However, its use is limited due to its extreme volatility. In the present study, we have synthesized and characterized a series of six new DADS analogs and investigated their interactions with different DNA duplexes. The spectroscopic and circular dichroism (CD) analyses revealed that DADS analogs bind preferentially with GC rich sequences. Thermodynamic parameters suggest that DADS analogs stabilize the calf thymus (CT) DNA and GC rich duplex by favorable enthalpic gains and follow the hierarchy, $d(GC)_7$ > CT DNA > $d(AT)_{10}$. Further, DADS analogs are less toxic and equally effective as the statins. The analogs therefore have a good potential to provide a new therapeutic approach for the treatment of cardiovascular and related diseases.

1. Introduction

Controlling gene expression with small DNA-binding molecules has been a challenge at the interface of medicinal chemistry and biology.[1–3] To achieve this goal, a number of chemical approaches have been investigated in search of small molecules (drugs) that can selectively bind to DNA and either activate or inhibit gene expression. This includes the examination of specific and non-covalent interactions, of small organic molecules, with DNA and RNA. The objective is to synthesize drugs that will act as specific modulators of gene activity.[4–6]

Chemical modification of bioactive components of medicinal plants is one of the most common approaches for drug discovery. These bioactive components can be modified by organic synthesis to prepare more stable and effective drugs (therapeutics).[7] Diallyldisulfide (DADS) is one of the major constituents of Garlic and has been shown to depress cholesterol synthesis by 10–25% at low concentration (<0.5 mmol/L).[8] The use of DADS is, however, limited due to its extreme volatility.[9] To overcome this limitation, our laboratory synthesized various derivatives of DADS that display greater hypolipidemic activity and enhanced stability, as compared to DADS. We have previously reported that the analogs with electron withdrawing substituents on the phenyl ring (compound **5**) showed antihyperlipidemic activity better than parent DADS and are comparable to that of Lovastatin.[10] These compounds modulate hepatic 3-hydroxy-3-methylglutaryl-CoA reductase[11] (HMGR) activity, principally by inhibiting the transcription of the HMGR gene, thereby reducing cholesterol levels, in an animal model (communicated elsewhere).

In this study, the synthesis and DNA-binding activity of a series of new DADS analogs are reported (Fig. 1). The DADS structure has been altered by chemical synthesis, and the analogs have been studied with respect to their affinity to DNA, their influence on DNA structure, and their cytotoxic effect on rat hepatocytes culture. In this work, we have employed various spectroscopic techniques such as UV spectroscopy, thermal denaturation, and circular dichroism (CD) to characterize DNA-binding activity of the DADS analogs and to analyze their sequence specificity. The thermodynamic parameters of DADS analogs/DNA complexes were determined by differential scanning calorimetry (DSC). The results conclusively prove the relationship between sequence selectivity,

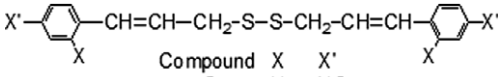

Compound	X	X'
5	H	NO_2
6	Cl	H
7	Cl	Cl
8	Br	H
9	Br	Br
10	H	F
11	H	CF_3

Figure 1. Structures of DADS derivatives **5**–**11** from the synthetic steps shown in Scheme 1.

* Corresponding author. Tel.: +91 11 27666272; fax: +91 11 27666248.
E-mail addresses: skrai7@gmail.com (S.K. Rai), manisha_07@hotmail.com (M. Tiwari).

0968-0896/$ - see front matter © 2008 Elsevier Ltd. All rights reserved.
doi:10.1016/j.bmc.2008.06.029

mode of binding, and the antihyperlipidemic activity of the DADS derivatives.

2. Results and discussion

2.1. Synthesis

The synthetic steps of the target compounds are shown in Scheme 1. The starting compound 2-mercaptoethanol (**1**) was oxidized with Br_2 to yield bis-(2-hydroxyethyl)disulfide(**2**) in the presence of $KHCO_3$. The compound (**2**) was brominated to the corresponding bis-(2-bromoethyl) disulfide (**3**) in the presence of 48% HBr and conc $H_2SO_4$with an approximate yield of 60%. Compound **3** was then converted to the corresponding phosphonium salt (**4**) by refluxing equimolar amounts of (**3**) and triphenylphosphine in dry DMF. The phosphonium salt thus obtained was refluxed for 24 h with appropriate aldehydes in the presence of sodium ethoxide to afford the DADS analogs (**5–11**) with an approximate yield of ~75% (Fig. 1). In our earlier publication, we have reported the use of lithium ethoxide for synthesizing the DADS analogs.[10] In the present study, we have modified the reaction by using sodium ethoxide, as lithium ethoxide tends to break the disulfide linkage, resulting in a lower yield. The product was purified by silica gel chromatography using ethyl acetate as the eluent to afford compounds **5–11**. The compounds (**5–11**) were fully characterized by spectroscopic analysis (mass, IR, and ^{1}H NMR).

2.2. DNA-binding properties

2.2.1. Absorption spectral analysis

It is a general observation that a hypochromic and red shift in the absorption spectra accompanies the binding of molecules to DNA. The extent of spectral change is related to the strength of binding.[12] In order to compare the DNA interactions of the DADS analogs, absorption titrations were conducted with calf thymus DNA (CT DNA) and with DNA duplexes of either alternating AT ($d(AT)_{10}$) or GC ($d(GC)_7$) sequences.

The spectral shifts and hypochromicities on complex formation of all analogs of DADS at drug/DNA ratio (r) of **5** are summarized in Table 1, and some important patterns can be observed for these complexes. There is insignificant red shift for the DADS analogs-$d(AT)_{10}$ and DADS analogs-CT DNA complexes, whereas a significant red shift (2–4 nm) is observed with DADS analogs-$d(GC)_7$ complexes. All the DADS analogs with CT DNA and $d(GC)_7$ duplex show hypochromicity of 18–22% and 28–34%, respectively, whereas $d(AT)_{10}$ duplex complexes have comparatively smaller hypochromicity (10–16%). Compound **6** shows the largest hypochromic shift with $d(GC)_7$. Large hypochromism and the red shift in the absorption spectra was an indication of a strong electronic interaction between the DADS analogs and the DNA bases (CT DNA and $d(GC)_7$). Our result also suggests that $d(AT)_{10}$ and $d(GC)_7$ duplexes behave differently on complex formation with DADS analogs.

2.2.2. Thermal melting analysis

UV-melting profiles of double-stranded DNAs in the presence of DADS analogs were performed at varying drug/DNA ratios. It is known that thermal denaturation profiles provide the simplest means for detecting binding and asserting relative binding strength.[12]

Natural genomic calf thymus DNA and two synthetic oligonucleotides with alternating AT ($d(AT)_{10}$) and GC ($d(GC)_7$) base pairs were chosen with the purpose of determining the possible sequence preferences of the tested compounds.

Table 2 summarizes the change in melting temperature (ΔT_m) of compounds (**5–11**) with CT DNA, $d(AT)_{10}$, and $d(GC)_7$ duplexes

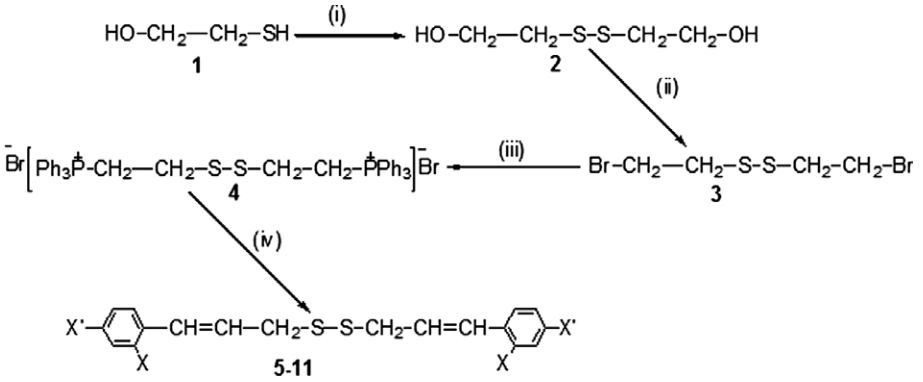

Scheme 1. Reagents and conditions: (i) Br_2, $KHCO_3$, DCM (49%); (ii) HBr, H_2SO_4 (59%); (iii) PPh_3, DMF, reflux (72%); (iv) NaOEt, substituted benzaldehyde (70–79%).

Table 1
Photometric properties of DADS analogs (**5–11**) with various DNA duplexes

DADS analogs	Calf thymus DNA		$d(GC)_7$		$d(AT)_{10}$	
	% Hypochromicity[a]	Red shift (nm) from 258	% Hypochromicity[a]	Red shift(nm) from 257	% Hypochromicity[a]	Red shift (nm) from 262
Compound **5**	21	1	30	3	16	0
Compound **6**	20	1	34	4	14	0
Compound **7**	22	0	29	3	15	0
Compound **8**	19	0	31	2	13	0
Compound **9**	18	1	28	4	12	0
Compound **10**	19	0	32	3	14	0
Compound **11**	20	0	29	3	10	0

[a] Titrations were conducted at constant duplex concentration (2.5 μM) with increasing drug concentration in 20 mM NaH_2PO_4/Na_2HPO_4 buffer (pH 7.4) containing 100 mM NaCl at room temperature. Values at saturating concentration of DADS analogs (12.5 μM).

Table 2
Effect of DADS analogs on thermodynamic parameters for drug/DNA complexes

Compound	T_m[a] (°C)	ΔT_m[b] (°C)	ΔH (kcal/mol)	$\Delta\Delta H$[b] (kcal/mol)	ΔS (cal/mol K^{-1})	$\Delta\Delta S$[b] (cal/mol K^{-1}	$\Delta G_{25^\circ c}$ kcal/mol	$\Delta\Delta G_{25^\circ c}$[b]
AT duplex	52	—	− 43.821	—	−141.61	—	−1.865	—
5	52	0	− 40.121	+3.6	−136.38	+5.2	+0.521	+2.3
6	49	− 3	− 32.809	+10.9	−125.14	+16.5	+4.401	+6.2
7	51	− 1	− 38.899	+4.9	−136.98	+4.6	+1.921	+3.7
8	52	0	− 36.201	+7.6	−129.11	+12.5	+2.273	+4.0
9	50	− 2	− 35.138	+8.6	−129.57	+12.0	+3.473	+5.3
10	51	− 1	− 36.188	+7.6	−131.93	+9.7	+3.127	+4.9
11	52	0	− 37.301	+6.5	−132.56	+9.1	+2.202	+4.0
GC duplex	87	—	−59.637	—	−162.757	—	−11.141	—
5	94	+7	− 63.754	−4.15	− 169.028	−6.2	−13.384	−2.2
6	93	+6	− 68.795	−9.19	− 186.52	−23.7	−13.212	−2.1
7	93	+6	− 62.758	−3.15	− 167.69	−4.9	−12.786	−1.6
8	92	+5	− 64.694	−5.09	− 175.602	−12.8	−12.364	−1.2
9	93	+6	− 61.567	−1.9	− 166.178	−3.4	−12.045	−0.9
10	92	+5	− 62.080	−2.48	− 167.41	−4.6	−11.893	−0.7
11	91	+4	− 60.746	−1.14	− 165.892	−3.1	−11.310	−0.2
CT DNA	73	—	−7.501	—	−20.824	—	−1.408	—
5	80	+7	−14.735	−7.2	− 41.980	−21.2	− 2.224	−0.8
6	81	+8	−15.656	−8.1	− 43.336	−22.5	− 2.271	−1.3
7	81	+8	−15.361	−7.8	− 44.175	−23.3	− 2.196	−0.8
8	80	+7	−13.234	−5.7	− 38.07	−17.2	− 1.889	−0.5
9	81	+8	−14.995	−7.5	− 42.647	−21.8	− 2.286	−0.8
10	79	+6	−10.694	−3.2	− 30.001	− 9.2	− 1.753	−0.3
11	78	+5	− 9.963	−2.4	− 27.748	− 6.9	−1.694	−0.2

[a] Experiments were carried out in PBS buffer, pH 7.4, containing 100 mM NaCl as described in Section 4.
[b] Changes due to drug–DNA complexes. The changes are calculated using non-rounded values of the thermodynamic parameters. A quantitative estimate of the binding parameters was obtained by subtracting the values describing the thermal transition of pure DNA from those derived for the drug–DNA. Complexes: $\Delta\Delta H = \Delta H - H_o$, $\Delta\Delta S = \Delta S - \Delta S_o$, $\Delta\Delta G = \Delta G - \Delta G_o$ (the zero index relates to pure DNA).

at a saturating concentration of DADS analogs ($r = 5$, 'r' refers to DADS analogs/ DNA ratio). As evident from Table 2, binding of any of the compounds with CT DNA resulted in T_m being raised, indicative of stabilization of CT DNA duplex. As the 'r' increases from 0 to 5, the thermal stabilities of CT DNA increase concomitantly. Inspection of Table 2 reveals that compounds **5**, **8**, and **11** have no effect on the melting temperature, whereas compounds **6** (Fig. 2A), **7**, **9**, and **10** decrease the T_m of the d(AT)$_{10}$ by 3 °C, 1 °C, 2 °C, and 1 °C, respectively. Further inspection of Table 2 and Figure 2B reveals that all the compounds show an increase in the melting temperature of the GC duplex. As the drug/DNA ratio increases from 0 to 5, the thermal stabilities of GC duplex increase by 4–7 °C. Compound **5** has the most stabilizing effect on the d(GC)$_7$. These results suggest that DADS analogs preferentially bind to GC base pairs rich regions of double-stranded DNA. These results are also comparable to those obtained for Daunomycin–DNA[13] and Crytolepin-DNA interaction,[14] which are known intercalators.

2.2.3. Circular dichroism (CD)

The melting experiments have provided us with useful information on the stability of drug–DNA duplexes; however, little can be discerned about the physical structure and mode of drug–DNA interactions from these experiments. CD spectropolarimetry provides a second means of detecting and characterizing ligand binding. Binding of an achiral molecule within a chiral environment, such as that afforded by right handed double helical DNA, can lead to induced optical activity for the bound species (ligand).[15] This is manifested in the appearance of a CD absorption band, assignable to the ligand but observed only in the presence of DNA. Panels A–C of Figure 3 show the representative CD spectra from 200 nm to 340 nm obtained by incremental titrations of compound **6** into CT DNA (panel A), d(GC)$_7$ (panel B), and d(AT)$_{10}$ (panel C) dissolved in an appropriate buffer.

As displayed in Figure 3A, a maximum (positive CD) at 280 nm and a minimum (negative CD) at 250 nm are induced when compound **6** is bound to CT DNA. The intensities of the induced

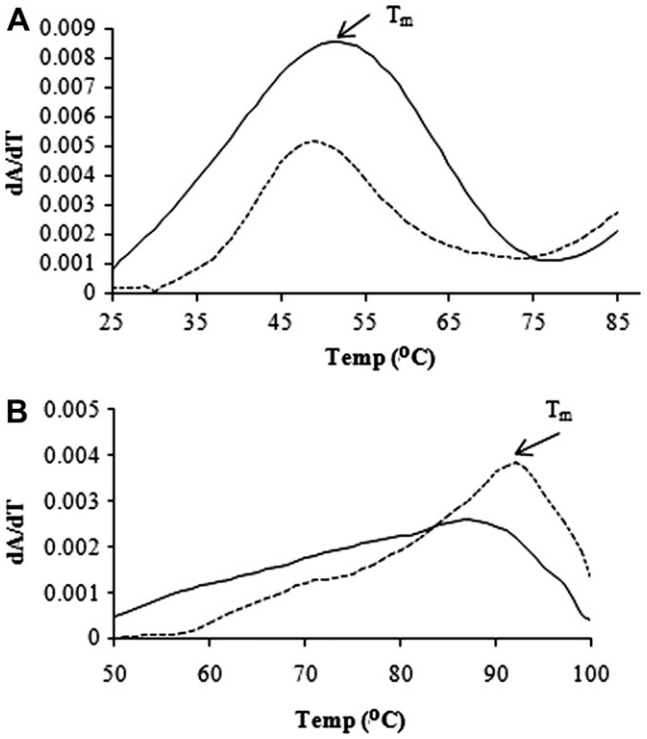

Figure 2. Derivative plot (T_m) for the d(AT)$_{10}$ (A) and d(GC)$_7$ (B) duplexes (solid lines) containing a compound **6** (dashed lines, respectively). The concentration of the d(AT)$_{10}$ and d(GC)$_7$ duplexes was 2.5 μM and compound **6** was 12.5 μM ($r = 5$). Melting temperature measurements were performed in 20 mM NaH_2PO_4/Na_2HPO_4 buffer (pH 7.4) containing 100 mM NaCl.

CD signals at 280 nm and 250 nm depend on the ratio of drug to DNA. The induced CD signals around 280 nm increase with the increase in ratio of drug to DNA. These spectral changes are an important evidence for the interaction of the drugs with the base pairs of CT DNA.[16] Since DADS derivatives are achiral molecules,

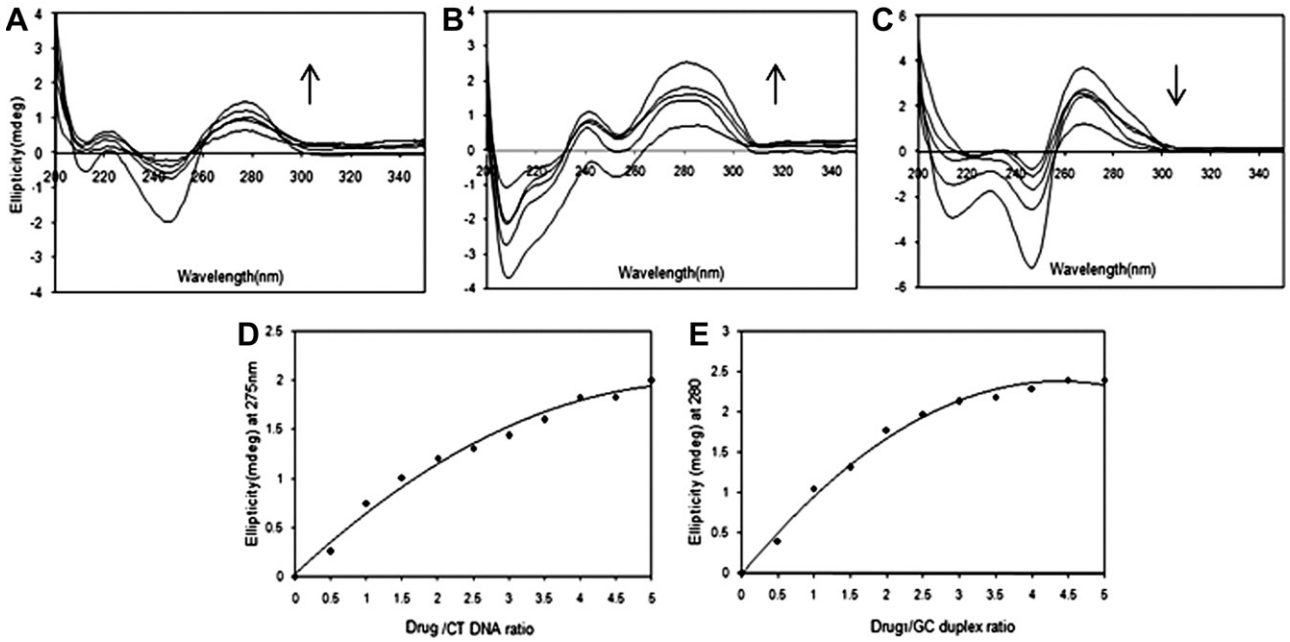

Figure 3. CD spectra showing the binding of compound **6** to calf thymus DNA (A), $d(GC)_7$ (B), and $d(AT)_{10}$ (C). The drug/DNA ratios were 0, 1.0, 2.0, 3.0, 4.0, and 5.0. CD titration plots and best-fit curves for the compound **6** binding to calf thymus DNA (D) and $d(GC)_7$ (E). Measurements were performed in 20 mM NaH_2PO_4/Na_2HPO_4 buffer (pH 7.4) containing 100 mM NaCl.

optical activity is generated in the asymmetric environment of the DNA double helix and this induced CD signal is considered to arise from the interaction of the transition moment of the chromophore (DADS analogs) with the transition moment of the chirally disposed surrounding DNA bases. The CD spectrum of DADS–CT DNA complex is similar to that of some other intercalators such as 9 aminoacridine, Daunomycin, and Nogalomycin.[17]

Ligand (Induced CD) spectra of DADS derivatives with $d(GC)_7$ duplex differ significantly from that of $d(AT)_{10}$ duplex. CD analyses of Compound **6** binding to GC duplex have shown the presence of induced cotton effect signal at 240 nm region (Fig. 3B). The variation in molar ellipticities around 240 nm regions at increasing drug/DNA ratio displayed first a negative signal which then becomes positive. These signals demonstrate that DADS analogs bind to GC rich DNA. Inspection of Figure 3C reveals that with compound **6**, AT duplex does not show any induced CD signal. Moreover, the maxima (at 270 nm) intensity gradually decreases with increasing concentration of '*r*'. At higher drug/DNA ratio (5:1), there is large negative intensity at 250 nm. Since the CD signal around 220–240 nm is characteristic of the DNA bound DADS analogs and positive CD bands were not observed with AT rich duplex, we can conclude that this is indicative of an intercalative mode of binding of the analogs, in GC rich regions of DNA.[18] Other analogs showed the same spectral behavior as that of compound **6**.

Single wavelength titration curve extracted from CD titration spectra of compound **6** binding to CT DNA and $d(GC)_7$ is depicted in Figure 3D and E, respectively. Here, '*r*' (DADS/duplex ratio) values provide estimate for apparent number of base pairs influenced by each event.[19] The ellipticity values at 280 nm (CT DNA) and 275 nm ($d(GC)_7$) were plotted against the compound **6**/duplex ratios. The slopes for $d(GC)_7$ were steep, and reached a plateau within the tested range of drug concentrations. On the other hand, the slopes obtained for CT DNA were gentle, and the increase in the signal intensity persisted at the high drug concentrations in these cases. The DADS analogs binding to each duplex were analyzed by curve fitting of the CD titration data. Analysis of the results shows that CT DNA shows apparent binding site size ('*n*') of 2.3–2.5 with all the DADS analogs, whereas $d(GC)_7$ has a binding site size of 2.4–2.6. The obtained '*n*' value suggested that at least two DADS molecules bound to these duplexes.

2.2.4. Binding affinity analysis

We have used UV-derived T_m data to obtain a quantitative estimate of binding constants, which is a direct measure of drug apparent binding affinity.[20,21] The enthalpy (dH_{wc}) of CT DNA and GC duplex melting was determined by DSC (Table 2). Eq. (1) was used to obtain the binding constant of the drug at the DNA melting temperature, in the presence of saturating concentration of the drug (12.5 μM). A value of '*n*' used in Eq. (1) is based on the size of drug binding site determined by CD titration spectra.[15] Our results indicate that compound **6** exhibits greater binding affinity for CT DNA ($K_{Tm} = 4.027 \times 10^5\ M^{-1}$) and $d(GC)_7$ ($K_{Tm} = 6.9 \times 10^6 M^{-1}$), whereas compound **11** shows the least binding affinity with $d(GC)_7$ ($\sim 10^2$). Specifically, we find the following hierarchy for DADS analogs binding to various duplexes (data not shown);

$$d(GC)_7 > \text{CT DNA} > d(AT)_{10}$$

This result is also consistent with our findings of thermal denaturation and CD titration data that all tested DADS analogs showed remarkable preference for alternating GC sequence, binding more efficiently to these than to natural CT DNA or AT rich sequences.

2.2.5. Thermodynamic profile

Differential scanning calorimetry (DSC), which is an informative method of obtaining direct data on thermal stability of drug–DNA complexes, was employed to characterize the influence of the DADS analogs on the thermal stability and energetics of CT DNA, $d(AT)_{10}$, and $d(GC)_7$ duplexes.[22] The melting enthalpy, ΔH_{melt}, of nucleic acid complexes with either groove binding or intercalating ligands is higher than ΔH_{melt} of pure nucleic acids, whereas the entropy of ligand binding (ΔS_{bind}) can have both positive and negative values, which mainly results from changes in the environment of the hydrated structure of the ligand–nucleic acid complex relative to the free nucleic acid.[23] The thermodynamic parameters of the DNA duplexes and its complexes with DADS ana-

logs, calculated using equations, described in section materials and methods, are summarized in Table 2.

The thermodynamic origin of stabilization of DADS analogs–DNA complex is both enthalpic and entropic driven. All the DADS analogs showed favorable free energy of binding with CT DNA and GC duplexes (CT DNA, $\Delta\Delta G = -0.2$ to -1.3 kcal/mol and $d(GC)_7$, $\Delta\Delta G = -0.2$ to -2.2 kcal/mol). This favorable free energy of binding was derived from a large negative enthalpy contribution (CT DNA, $\Delta\Delta H = -2.4$ to -8.1 kcal/mol and $d(GC)_7$, $\Delta\Delta H = -1.14$ to -9.19 kcal/mol, Figure 4B) but was opposed by the entropic contribution (CT DNA, $\Delta\Delta S = -6.9$ to -23.3 cal/mol K^{-1} and $d(GC)_7$, $\Delta\Delta S = -3.1$ to 23.7 cal/mol K^{-1}). Hence, the enthalpy term is favorable for interaction whereas entropy term is unfavorable, which is probably due to the more ordered structure of the hydration environment of drug–DNA complexes compared to that of pure DNA.[23] Hence, DADS analogs stabilize the duplexes by favorable enthalpic gains.

Closer examination of Table 2 reveals that all the $d(AT)_{10}$–DADS analogs complexes exhibit positive $\Delta\Delta H$ value, that is, enthalpy effects destabilize the duplex (Fig. 4A). It may be possible that DADS analogs disrupt the stacking and H-bonding interaction of neighboring AT bases or may be an effect of hydrophobic DADS analogs being forced in juxtaposition to highly charged DNA.[24] These destabilizing effects are counter balanced by positive $\Delta\Delta S$ values ($d(AT)_{10}$, $\Delta\Delta S = +4.6$ to $+16.5$ cal/mol K^{-1}), which stabilize the duplex.

Our results suggest that DADS analogs, when interact with CT DNA and $d(GC)_7$, stabilize the duplex by favorable enthalpic gains and may interact in similar fashion but differently with AT duplex. Thus, the order of thermodynamic stabilization for these compounds is

$$d(GC)_7(\mathbf{5} > \mathbf{6} > \mathbf{7} > \mathbf{8} > \mathbf{9} > \mathbf{10} > \mathbf{11}) > \text{CT DNA}(\mathbf{6} > \mathbf{5} \approx \mathbf{7} \approx \mathbf{9} > \mathbf{8} > \mathbf{10} > \mathbf{11}) > d(AT)_{10}$$

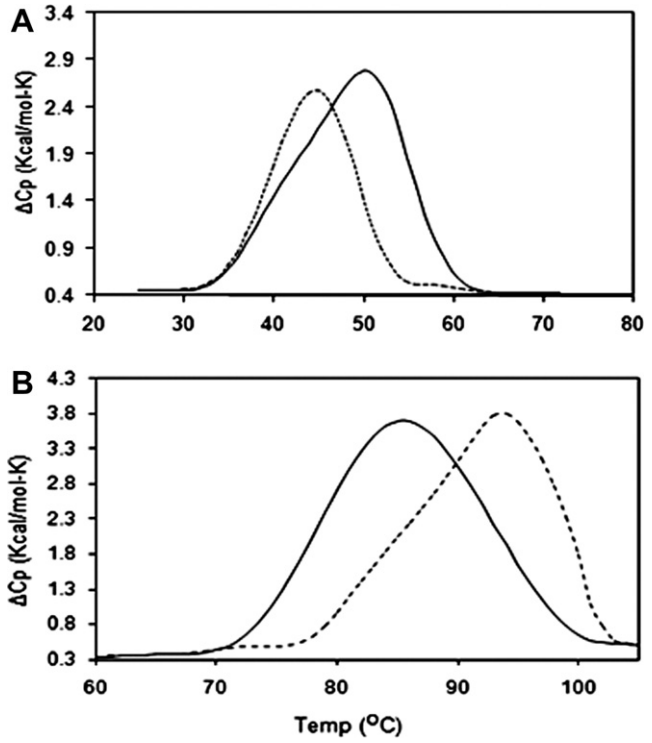

Figure 4. DSC thermograms for the $d(AT)_{10}$ (A) and $d(GC)_7$ (B) duplexes(solid lines) containing a compound **6** (dashed lines, respectively). The concentrations of the $d(AT)_{10}$ and $d(GC)_7$ duplexes were 100 μM, and the buffer conditions were 20 mM sodium phosphate, pH 7.4 and 100 mM NaCl.

Hence, from the results of thermodynamic parameters, it is evident that compounds **5** forms the most stable complexes with $d(GC)_7$ duplex. This result also shows that DADS analogs have more specificity toward GC rich DNA.

2.3. Cytotoxicity of DADS analogs against primary rat hepatocytes

The in vitro cytotoxicity of DADS derivatives was evaluated using MTT method.[25] The IC_{50} values (cytotoxicity potency indices) of DADS analogs (**5–11**) against primary rat hepatocytes in culture are summarized in Table 3. After 24 h incubation, increasing concentrations of DADS analogs (1–1000 μM) led up to a gradual decrease of the fraction of surviving cells in a dose dependant manner (20–98%). The DADS analogs exhibited low or insignificant cytotoxicity with high IC_{50} values. Among the derivatives, compound **11** was found to be most potent in inhibiting the cell proliferation with the lowest IC_{50} value of 140 μM suggesting that the substitution on phenyl ring with fluoro or trifluoro methyl groups leads to considerable increase in cytotoxicity. On comparison with different statins, we have found the DADS analogs to be less cytotoxic than the statins, such as Lovastatin (IC_{50} = 90 μM), Atorvastatin (125 μM), Simvastatin (>100 μM) in primary rat hepatocyte culture.[26]

2.4. Effect of DADS analogs on serum and hepatic lipid content

Hypercholesterolemia was induced in rats by feeding them a cholesterol rich diet for 2 weeks (5% cholesterol) (Table 4). An atherogenic diet induced a marked increase in serum as well as triglycerides levels ($p < 0.001$). At the end of the study, animals treated with DADS analogs (Group V–XI) showed significantly lower levels of serum and hepatic cholesterol with respect to hypercholesterolemic rats. DADS analogs also reduced the triglycerides levels significantly ($p < 0.001$) with respect to hypercholesterolemic rats (Group II). Compounds **5** and **6** showed the maximum diminution in serum and hepatic cholesterol as well as in triglycerides levels with respect to hypercholesterolemic rats, and these antihyperlipidemic properties were found to be comparable to that of Lovastatin treated hypercholesterolemic rats.

3. Conclusion

In this paper, we report the synthesis and characterization of six new analogs of DADS, by ^{1}H NMR and mass spectroscopy. To further evaluate their potential pharmaceutical properties, the DNA-binding activity has been investigated by absorption, circular dichroism, and DSC measurements. The experimental results indicate that DADS analogs bind to GC rich regions of DNA duplexes.

Spectrophotometric titrations suggest that there is large hypochromic shift, moderate red shift and substantial increase in the thermal denaturation temperature, when DADS analogs bind to CT DNA and $d(GC)_7$ duplexes. DADS analogs which do not possess

Table 3
IC_{50} cytotoxicity values (μM) of DADS derivatives against primary rat heptocytes (data derived from the mean of three independent assays)

Compound	Rat hepatocyte culture (IC_{50}, μM)
5	335
6	425
7	350
8	365
9	275
10	155
11	140

Table 4
Effect of Lovastatin, Allicin, and DADS analogs on the lipid profile of experimental rats[a]

Lipid(mg/dl)	Group I	Group II	Group III	Group IV	Group V	Group VI	Group VII	Group VIII	Group IX	Group X	Group XI
Cholesterol											
Hapatic	1.92 ± 0.2	2.76 ± 0.04†††	2.15 ± 0.97††	1.6 ± 0.35***	1.97 ± 0.01**	1.87 ± 0.24**	2.04 ± 0.9**	2.07 ± 0.56**	2.12 ± 0.72**	2.07 ± 0.89**	2.12 ± 0.64**
Serum	41.34 ± 0.95	54.05 ± 1.10††	42.69 ± 0.65††	36.21 ± 0.71***	38.37 ± 0.62**	37.29 ± 0.86**	42.15 ± 0.89**	41.07 ± 0.6**	41.61 ± 0.74**	42.15 ± 1.61**	42.69 ± 0.99**
Triglyceride											
Hepatic	20.00 ± 0.48	27.13 ± 0.73††	20.34 ± 0.39**	17.35 ± 0.19***	19.8 ± 0.41**	19.28 ± 220**	20.61 ± 1.10**	21.41 ± 0.76**	21.79 ± 0.92**	21.03 ± 1.08**	20.57 ± 1.76**
Serum	34.99 ± 1.02	44.43 ± 1.14†	36.86 ± 0.43***	31.98 ± 0.82***	33.32 ± 0.89*	32.87 ± 0.95*	34.65 ± 1.49*	35.54 ± 0.87*	34.65 ± 0.76*	35.54 ± 0.858*	35.09 ± 1.17*

[a] Group I, saline fed rats; Group II, rats fed with 5% cholesterol; Group III, rats fed with 5% cholesterol along with oral administration of Allicin; Group IV, rats fed with 5% cholesterol along with oral administration of Lovastatin; Group 'V–XI', rats fed with 5% cholesterol along with oral administration of compounds **5–11**, respectively. Data are presented as means ± SE obtained from duplicate assay on every treatment.

* $p < 0.05$.
** $p < 0.01$.
*** $p < 0.001$ as compared to Group II.
† $p < 0.05$.
†† $p < 0.01$.
††† $p < 0.001$ as compared to Group I.

intrinsic optical activity become optically active when bound to DNA (CT DNA and $d(GC)_7$ duplex) and exhibit a CD spectrum similar to known intercalators. The thermodynamic profile demonstrates that compounds **5** and **6** have the most stabilizing effect on GC rich DNA which is predominantly enthalpy driven. Our MTT assay revealed that compounds **5** and **6** showed minimal toxic effect in primary rat heptocytes culture, whereas compound**11** shows the least IC_{50} value as well as the most destabilizing effect on DNA duplexes.

All the results discussed above are also consistent with the antihyperlipidemic properties of these DADS compounds evaluated by biochemical determinations. The compounds **5** and **6**, thus, seem to be well suited for further work aiming at the development of new antihyperlipidemic agents, which can act as specific modulators of gene activity (HMGR gene).

4. Experimental

4.1. General

All organic solvents and common reagents were procured from the Merck India Ltd. All the derivatives of benzaldehyde and Sodium metal were procured from Aldrich Chemical Company, Inc. USA. TLC was carried out on commercially available flexible TLC silica gel (silica gel 60 F254) plates (E Merck, Germany). The purity of all organic compounds was confirmed by TLC, ^{1}H NMR, IR, and Mass. ^{1}H NMR spectra were recorded in Bruker Spectrospin Avance 300 instrument operating at 300 MHz in $CDCl_3$ or DMSO using TMS as an internal standard. IR spectra (KBr) were recorded on a Perkin-Elmer BX FT-IR instrument. Melting points were determined on a Buchi melting point B-450 instrument. Mass spectra were recorded on a Qstar (Appllied biosystem) ESI-MS mass spectrometer.

Absorption spectra were determined using Cary varian-300 spectrophotometer. Oligodeoxynucleotides and calf thymus DNA (CT DNA) were purchased from Sigma–Aldrich Chemical Pvt Ltd (USA). CT DNA solution was prepared by swelling it (1 mg/ml) overnight at 4 °C in phosphate buffer, then filtering and adjusting the concentration to the desired value with buffer. An extinction coefficient of 6600 M^{-1} cm^{-1} has been used. The alternating AT (20 bp, $d(AT)_{10}$) and GC (14 bp, $d(GC)_7$) self-complementary oligomer duplexes were used for the determination of sequence specificity. Their concentration was determined using a molar extinction coefficient of 217.8 mM^{-1} cm^{-1} and 136.8 mM^{-1} cm^{-1} for $d(AT)_{10}$ and $d(GC)_7$ oligomer duplex, respectively. For experiments involving UV spectroscopy and circular dichroism, titrations of the drug with DNA, at different drug/DNA ratios ('r'), were performed with fixed DNA concentration (2.5 μM) and increasing concentrations of the drug substrates from 0 μM to 12.5 μM, until no further changes in drug–DNA spectra were observed. All the measurements were performed in 20 mM sodium phosphate (NaH_2PO_4/Na_2HPO_4) buffer containing 100 mM of NaCl, pH 7.4. The absence of precipitates or changes in the absorption spectra of the stock solutions was regularly verified.

4.2. Synthesis of bis-(2-hydroxy ethyl) disulfide (2)

To a solution of dichloromethane (40 ml) 3 ml (40 mM) of 2-mercaptoethanol (**1**) was added. To this, 40 ml of 10% aqueous potassium hydrogen carbonate ($KHCO_3$) and a solution of 2 ml Bromine (40 mM) in 10 ml dichloromethane was added to the reaction vessel whereupon the color of bromine disappeared during addition. The mixture was stirred and cooled in ice water bath. The organic phase was separated, and the aqueous phase was extracted with (3× 10 ml) dichloromethane. The organic phases were combined and dried with anhydrous Na_2SO_4. The solvent was evapo-

rated, and the compound was further purified by column chromatography. (1 g, 48.8%); IR (KBr, cm^{-1}): 3330 (O–H str.), 2925 (C–H str.), 696 (C–S str.); ^1H NMR (300 MHz; $CDCl_3$): δ 2.88 [t, $2 \times 2H(a)$, J = 1.05 Hz]; 2.99[s, $2 \times 1H$ (OH)]; 3.89 [t, $2\times$ 1H(b), J = 1.05 Hz]; MS($C_4H_{10}O_2S_2$): m/e 154 (M^+), 92(100).

4.3. Synthesis of bis-(2-bromoethyl)disulfide (3)

To a solution of 48% HBr (70 ml) 46 ml of concd H_2SO_4 was added with continuous stirring. The flask was pre-cooled in an ice bath, and to the resulting ice-cold solution 2 g of compound **2** was added dropwise. The reaction mixture was left to stir for 24 h at room temperature. After this the reaction mixture was heated for 3 h on a steam bath. Dichloromethane (10 ml) was added to the reaction mixture. The upper layer was taken, washed with water, 10% Na_2CO_3 solution, and then dried over anhydrous Na_2SO_4. The dichloromethane was evaporated, and the desired compound **3** was obtained. (2 g, 59%): IR (KBr, cm^{-1}); 617 (C–S str.), 563 (C–Br str.), 445 (–S–S str.): ^1H NMR (300 MHz; $CDCl_3$); δ 2.95 (t, $2 \times 2H(a)$, J = 1.0 Hz); 3.67(t, $2 \times 2H(b)$, J = 1.0 Hz): MS ($C_4H_8Br_2S_2$): m/e 280 (M^+).

4.4. Conversion of (3) to the analogous phosphonium bromide (4)

To a solution of compound **3** (2.8 g, 0.01 mmol) in dry dimethylformamide (15 ml) triphenyl phosphine (5.5 g, 0.02 mmol) was added under nitrogen, and the mixture was refluxed for 5 h. The mixture was allowed to cool to room temperature, and 15 ml of hexane was added. The desired phosphonium salt precipitated out. The solution was filtered, washed with hexane, and dried. White crystals of (**4**) were obtained (5.6 g, 71.7%): Mp, 130–132 °C: IR (KBr, cm^{-1}); 3053 (C–H str.), 691 (C–S str.): ^1H NMR (300 MHz, $CDCl_3$); δ 3.00 (t, $2 \times 2H(a)$, J = 2.82 Hz); 3.75 (t, $2 \times 2H(b)$, J = 3.66 Hz); 7.05–7.45(s, $6 \times 5H$). MS($C_{40}H_{38}Br_2P_2S_2$): m/e 804 (M+).

4.5. General procedure for the preparation of 5–11

To a stirred solution of compound **4** in super-dry ethanol appropriate substituted benzaldehyde (2 mM) was added in the presence of sodium ethoxide (formed by the addition of sodium, 25 mM, in super-dry ethanol). The reaction was set up in absolute dry condition by flushing Nitrogen gas. The mixture was stirred at the reflux temperature for 24 h. The reaction mixture was then poured into ice. The product precipitated out and was filtered. The residue was purified by column chromatography and elution with hexane/ethyl acetate (80:20).

4.5.1. Conversion of 4 to bis[3-(4′-nitrophenyl)prop-2-ene]-disulfide (5)

An organic solid. Yield; 78.6%: Mp 140–142 °C: IR (KBr, cm^{-1}); 3055 (C_{sp2}–H str.), 2948 (C_{sp3}–H str.), 1583 [–N=O str. (anti)], 1388 cm^{-1} [–N=O str. (sym)], 690 (C–S str.): ^1H NMR ($CDCl_3$); δ 1.83 [d, $2 \times 2H(a)$, J = 1.87 Hz]; 6.00[m, $2 \times 1H(b)$]; 6.30 [d, $2 \times 1H(c)$ J = 1.83]; 6.92–7.35(m, 8H, aromatic protons): MS($C_{18}H_{16}N_2O_4S_2$): m/e 380 (M^+). Compound **5** is the same as that reported previously, as the spectral data are all identical.[6]

4.5.2. Conversion of 4 to bis[3-(2′-chlorophenyl)prop-2-ene]-disulfide (6)

Yellow solid. Yield: 77.0%: Mp −115 to 117 °C: IR (KBr, cm^{-1}); 3048 (–C_{sp2}–H str.), 2930 (–C_{sp3}–H str.), 1623 (–C=C str.), 477 (–S–S str.), 691(–C–S–str.), 670 (–C–Cl–str.): ^1H NMR (300 MHz,$CDCl_3$); δ 1.25[s, $2 \times 2H(a)$]; 4.78[s, $2 \times 1H(b)$]; 5.29 [s, $2 \times 1H(c)$]; 7.21–7.49 (m, $2 \times 4H$, aromatic protons): MS ($C_{18}H_{16}Cl_2S_2$): m/e 367 (M^+).

4.5.3. Conversion of 4 to bis[3-(2,4′-dichlorophenyl)prop-2-ene]disulfide (7)

An orange solid compound. Yield; 77.8%: Mp 155–157 °C: IR (KBr, cm^{-1}): 3048 (-C_{sp2}–H str.), 2930(-C_{sp3}–H str.), 1623 (–C=C str.), 477 (–S–S str.), 691(–C–S str.), 670 (–C–Cl str.):^1H NMR (300 MHz, $CDCl_3$); δ 1.18 [s,$2 \times 2H(a)$]; 4.86–4.89 [m, $2 \times 1H(b)$]; 5.22–5.29[m, $2 \times 1H(c)$]; 7.35–7.61(m, 3H, aromatic protons): MS($C_{18}H_{14}Cl_4S_2$): m/e 435 (M^+).

4.5.4. Conversion of 4 to bis[3-(2′-bromophenyl)prop-2-ene]-disulfide (8)

Yield: 190 mg (72.3%): Mp −220 to 224 °C: IR (KBr, cm^{-1}); 3055 (–C_{sp2}–H str.); 2927 (–C_{sp3}–H str.), 1685 (–C=C str.); 427(–S–S str.); 691(–C–S str.), 560 (–C–Br str.): ^1H NMR ($CDCl_3$): δ1.66[s, $2 \times 2H(a)$]; 4.00–4.23 [m, $2 \times 1H(b)$]; 4.77[s, $2 \times 1H(c)$]; 7.26–7.34 (m, $2 \times 4H$, aromatic protons): MS($C_{18}H_{16}Br_2S_2$); m/e 455 (M^+).

4.5.5. Conversion of 4 to bis[3-(2,4′-dibromophenyl)prop-2-ene]disulfide (9)

Yield: 190 mg (79.2%): Mp −100 to 130 °C: IR (KBr, cm^{-1}); 3046 (C_{sp2}–H str.); 3005 (broad band); 2936 (–C_{sp3}–H str.), 1685 (–C=O str.); 690(–C–S str.), 560 (–C–Br str.): ^1H NMR (300 MHz, $CDCl_3$); δ1.85 [d, $2 \times 2H(a)$, J = 1.60 Hz]; 6.08 [m, $2 \times 1H(b)$]; 6.38 [$2 \times 1H(c)$]; 7.02–7.48 (m, 8H, aromatic protons): MS ($C_{18}H_{14}Br_4S_2$); m/e 615 (M^+).

4.5.6. Conversion of 4 to bis[3-(4′-fluorophenyl)prop-2-ene]-disulfide (10)

Yield: 76.5%: Mp −145.67 °C: IR (KBr, cm^{-1}): 3435 (O–H str.); 3054(–C_{sp2}–H str.), 2918(–C_{sp3}–H str.); 691(–C–S str.), 1100(–C–F str.): ^1H NMR (300 MHz, $CDCl_3$); δ1.41 [t, $2 \times 2H(a)$, J = 1.77 Hz]; 4.00–4.09 [m, $2 \times 1H(b)$]; 4.61–4.67 [m, $2 \times 1H(c)$]; 6.89 [d, $2 \times 2H(d)$, J = 8.49 Hz]; 7.29 [d, $2 \times 2H(e)$, J = 7.95]: MS ($C_{18}H_{16}F_2S_2$): m/e 335 (M^+).

4.5.7. Conversion of 4 to bis[3-{(4′-trifluoromethyl)phenyl}-prop-2 ene]disulfide (11)

Yield: 70%: Mp −184 to 186 °C: IR (KBr, cm^{-1}); 3435(O–H str.); 3054(–C_{sp2}–H str.), 2918(–C_{sp3}–H str.); 691(–C–S str.), 610 (–C–F str.): ^1H NMR (300 MHz, $CDCl_3$); δ1.66 [s, $2 \times 2H(a)$]; 4.71–4.79 [m, $2 \times 1H(b)$; 5.06–5.30 [m, $2 \times 1H(c)$]; 7.21–7.68 (m, $2 \times 4H$, aromatic protons): MS ($C_{20}H_{16}F_6S_2$); m/e 435 (M^+).

4.6. Spectrophotometric titrations

Titration of the drugs with DNA covering a large range of DNA–phosphate/drug ratios was performed by keeping the DNA concentration constant and varying the concentration of the analogs of DADS. Initial concentrations of DNAs and DADS analogs were kept as 2.5 μM and 0 μM, respectively. The experiments were conducted at 25 °C in phosphate buffer (pH 7.4) containing 100 mM NaCl. After mixing, the solution was allowed to stand for 15 min, the corresponding absorption spectra in the region from 200 nm to 340 nm were measured at room temperature.

4.7. T_m measurements

The thermal denaturation experiments were performed on a Varian make CARY-100 Spectrophotometer equipped with a peltier thermo-programmer and interfaced with a Pentium III computer for data collection and analysis. The temperature dependence on the absorption value of the DNA was monitored at 260 nm. The

temperature of the cell holder was increased from 25 °C to 100 °C at a rate of 1 °C/min. A teflon-coated temperature probe, immersed directly in a control cuvette, measured the sample temperature. The sample solutions were overlaid with paraffin-oil to prevent evaporation. The melting temperature (T_m) was taken to be the midpoint of the hyperchromic transition determined from first derivatives plots. All ΔT_m values are reported as the means from at least three determinations. The accuracy of the reported T_m values is ±0.5 °C. The duplexes were dissolved in the buffer containing 20 mM sodium phosphate (NaH_2PO_4/Na_2HPO_4), pH 7.4 and 100 mM NaCl.

4.8. Circular dichroism (CD)

CD Spectra were recorded on JASCO-715 Spectropolarimeter interfaced with an IBM PC compatible computer, calibrated with D-Camphor sulphonic acid. Five scans of the spectrum were collected over the wavelength range of 220–340 nm at a scanning rate of 100 nm/min. The desired ratios of compound to DNA were obtained by adding compound to the cell containing a constant amount of DNA. The duplexes were dissolved in the buffer containing 20 mM sodium phosphate (NaH_2PO_4/Na_2HPO_4), pH 7.4 and 100 mM NaCl. The average of multiple scans was used for analysis. The scan of the buffer alone recorded at room temperature was subtracted from the average scans for each DNA duplex. Data were collected in units of millidegrees versus wavelength and normalized to total DNA concentration.

4.9. Determination of binding constants by thermal melting study

Profiles of absorbance at 260 nm versus temperature were measured between 25 °C and 100 °C, at a heating rate of 1 °C min^{-1}, in the presence of 100 mM of NaCl, in 20 mM sodium phosphate (NaH_2PO_4/Na_2HPO_4) buffer (pH 7.4) and saturating concentrations of DADS derivatives (2.5 μM DNA (bp); 12.5 μM DADS compounds). DNA melting temperatures (T_m) were used to calculate the binding constant to different DNA duplexes at the DNA melting temperature (K_{Tm}), using the equation derived by Crothers[20] and McGhee[21]:

$$1/T^{o}_{m} - 1/T_m = (R/ndH_{wc}) \ln(1 + K_{Tm}a) \quad (1)$$

where T^{o}_{m} is the UV-melting temperature of DNA duplex alone, T_m is the melting temperature in the presence of saturating amounts of the drug, dH_{wc} is the enthalpy of DNA melting obtained by DSC, R is the gas constant, K_{Tm} is the drug binding constant at T_m, 'a' is the free drug activity, which is estimated by one half of the total drug concentration, and 'n' is the size of the drug binding site.

4.10. Differential scanning calorimetry

Excess heat capacity (ΔC_p) versus temperature profiles for the thermally induced transitions of CT DNA, AT, and GC duplexes of DADS analogs were measured using a Pyris 6-DSC Calorimeter (Perkin-Elmer, USA). In the DSC experiments, the concentrations of the CT DNA, $d(AT)_{10}$, and $d(GC)_7$ duplexes were 100 μM, the heating rate was 60 °C/h and the maximum temperature was 100 °C. After reaching the maximum temperature the samples were cooled at the same rate to the starting temperature of 25 °C. Here, ΔC_p is defined as excess heat capacity, which is baseline subtracted and concentration normalized.[27] The reference scans were subtracted from the sample scans to obtain ΔC_p versus temperature profiles. Enthalpies (ΔH_{cal}) and entropies (ΔS_{cal}) of duplex melting were calculated from the areas under the experimental ΔC_p versus T ($\Delta H_{cal} = \int \Delta C_p dT$) and derived $\Delta C_p/T$ versus T curves ($\Delta S_{cal} = \int \Delta(C_p/T)dT$), respectively, using ORIGIN v.5.0 software (Microcal). The free energy of duplex formation at 25 °C (ΔG_{25}) was calculated using the standard thermodynamic relationship given in Eq. (2) and the corresponding ΔH_{cal} and ΔS_{cal} values:

$$\Delta G^{\circ}_{25} = \Delta H^{-}_{cal}(298.15)\Delta S_{cal}. \quad (2)$$

The duplexes were dissolved in the buffer containing 20 mM sodium phosphate (NaH_2PO_4/Na_2HPO_4), pH 7.4 and 100 mM NaCl.

4.11. Cell culture and cytotoxicity assay

Hepatocytes were isolated from rat liver as previously described.[28] Hepatocytes were collected and cultured in Dulbecco's modified Eagle's medium (DMEM) containing 10% fetal bovine serum in the Thermo Forma Direct Heat CO_2 incubator with 5% CO_2–95% O_2 at 37 °C. The effect of DADS analogs on the viability of the hepatocytes was determined by the MTT assay, which is based on the reduction of a tetrazolium salt by mitochondrial dehydrogenase in the viable cells.[25] The cells were seeded in a 96-well plate at a density of 1×10^5 cells/ml and treated with 1–1000 μM of DADS analogs. After incubation for 24 h at 37 °C, 50 μl of the MTT (Bio-Gene, USA) stock solution (2 mg/ml) was added to each well to attain a total reaction volume of 200 μl. After incubation for 4 h, the plate was centrifuged at 800g for 5 min and the supernatants were aspirated. The formazan crystals in each well were dissolved in 150 μl DMSO, and the A_{540} was read on a scanning multi-well spectrophotometer. All drug doses were tested in triplicate and the IC_{50} values were derived from the mean OD values of the triplicate tests versus drug concentration curves.

4.12. Animals and biochemical estimations

Adult male Wistar rats, weighing 100–120 g each, were selected from the stock colony maintained in our animal facility with daily light/darkness cycle 14–10 h, with free access to food and water. Experiments were performed according to the guidelines of the Institutional Animal Ethics committee. They were given standard sterilized commercial diet purchased from Brooke Bond India Ltd. The animals were then divided into eleven groups of six animals each. The control group received only rat chow and saline solution (Group I): Control hypercholesterolemic group were fed with 5% cholesterol in their diet for 2 weeks (Group II): The experimental groups (Group III–XI) were fed with 5% cholesterol for 1 week and then fed with cholesterol rich diet supplemented with Allicin, Lovastatin and different DADS analogs (Compounds **5**–**11**) in the second week (20 mg/Kgwt, suspension in water, po), respectively.[10] The animals were immediately dissected to remove their tissues, which were washed in ice-cold saline (0.85% NaCl). The extraneous material was removed. Approximately 1 g of tissue was kept for estimation of lipids and the remaining was used for biochemical assays. The levels of cholesterol (hepatic and serum) and triglycerides (hepatic and serum) were measured by standard enzymatic assays (Sigma Chemical Co., St. Louis, MO, USA).

Acknowledgments

The authors express their sincere gratitude to Prof. Vani Brahmachari and Dr. Shrikant Kukreti, for their valuable suggestions. The author S.K.R. thanks the Council of Scientific and Industrial Research (CSIR), India, for the award of JRF and SRF. The author M.T. thanks the Department of Science and Technology, Government of India, for financial support.

References and notes

1. Gottesfeld, J. M.; Turner, J. M.; Dervan, P. B. *Gene Expr.* **2000**, *9*, 77.
2. Dervan, P. B. *Bioorg. Med. Chem.* **2001**, *9*, 2215.

3. Gutierrez, A. J.; Matteucci, M. D.; Grant, D.; Matsumura, S.; Wagner, R. W.; Froehler, B. C. *Biochemistry* **1997**, *36*, 743.
4. Fox, K. R. *Drug–DNA Interaction Protocols*; Humana Press: Totowa, NJ, 1997.
5. Chaires, J. B. *Drug–Nucleic Acid Interactions*; Academic Press: New York, 2001.
6. Jiang, Z.-H.; Hwang, G.-S.; Xi, Z.; Goldberg, I. H. *J. Am. Chem. Soc.* **2002**, *124*, 3216.
7. Tan, J.-H.; Zhang, Q.-X.; Huang, Z.-S.; Chen, Y.; Wang, X.-D.; Gu, L.-Q.; Wu, J. Y. *Eur. J. Med. Chem.* **2006**, *41*, 1041.
8. Gebahardt, R.; Back, H. *Lipids* **1996**, *31*, 1269.
9. Cavallito, C. J.; Bailey, J. H. *J. Am. Chem. Soc.* **1944**, *66*, 1950.
10. Sharma, M.; Tiwari, M.; Chandra, R. *Bioorg. Med. Chem. Lett.* **2004**, *14*, 5347.
11. Goldstein, J. L.; Brown, M. S. *Nature* **1990**, *343*, 425.
12. Chaires, J. B.; Dattagupta, N.; Crothers, D. M. *Biochemistry* **1982**, *21*, 3933.
13. Kumar, C. V.; Asuncion, E. H. *J. Am. Chem. Soc.* **1993**, *115*, 8547.
14. Bonjean, K.; Pauw-Gillet, M. C.; Defresne, M. P. *Biochemistry* **1998**, *37*, 5136.
15. Nabiev, I.; Chourpa, J.-F.; Riou, C.; Nguyen, H.; Lavelle, F.; Manfait, M. *Biochemistry* **1994**, *33*, 9013.
16. Frederick, C. A.; Williams, L. D.; Ughetto, G.; Van der Marel, G. A.; Van Bboom, J. H.; Rich, A.; Wang, A. H.-J. *Biochemistry* **1990**, *29*, 2538.
17. Dalgleish, D. G.; Fey, G.; Kersten, W. *Biopolymers* **1974**, *13*, 1757.
18. Lyng, R.; Rodger, A.; Norden, B. *Biopolymers* **1991**, *31*, 1709.
19. Inase, A.; Kodama, T. S.; Sharif, J.; Xu, Y.; Ayame, H.; Sugiyama, H.; Iwai, S. *J. Am. Chem. Soc.* **2004**, *126*, 11017.
20. Crothers, D. M. *Biopolymers* **1971**, *10*, 2147.
21. Mchgee, J. D. *Biopolymers* **1976**, *15*, 1345.
22. Veselkov1, A. N.; Maleev, V. Y.; Glibin, E. N.; Karawajew, L.; Davies, D. B. *Eur. J. Biochem.* **2003**, *270*, 4200.
23. Lane, A. N.; Jenkins, T. C. *Q. Rev. Biophys.* **2000**, *33*, 255.
24. Moreira, B. G.; You, Y.; Behlke, M. A.; Owczarzy, R. *Biochem. Biophys. Res. Commun.* **2005**, *327*, 473.
25. Kang, K. A.; Lee, K. H.; Park, J. W.; Lee, N. H.; Na, H. K.; Surh, Y. J.; You, H. J.; Chung, M. H.; Hyun, J. W. *FEBS Lett.* **2007**, *581*, 2000.
26. Kubota, T.; Fujisaki, K.; Itoh, Y.; Yano, T.; Sendo, T.; Oishi, R. *Biochem. Pharmacol.* **2004**, *67*, 2175.
27. Leharne, S. A.; Chowdhry, B. Z. In *Biocalorimetry: Applications of Calorimetry in the Biological Science*; Wiley & Sons: Chichester, UK, 1998; p 157.
28. Page, D. T.; Garvey, J. S. *J. Immunol. Methods* **1979**, *27*, 159.